

Muon-to-Electron Conversion in Mirror Fermion Model with Electroweak Scale Non-Sterile Right-handed Neutrinos

P. Q. Hung^{1,4}, Trinh Le¹, Van Que Tran² and Tzu-Chiang Yuan^{3,5}

¹*Department of Physics, University of Virginia,*

Charlottesville, VA 22904-4714, USA

²*Department of Physics, National Taiwan Normal University, Taipei 116, Taiwan*

³*Institute of Physics, Academia Sinica, Nangang, Taipei 11529, Taiwan*

⁴*Center for Theoretical and Computational Physics,*

Hue University College of Education, Hue, Vietnam

⁵*Physics Division, National Center for Theoretical Sciences, Hsinchu, Taiwan*

(Dated: January 10, 2017)

Abstract

The muon-to-electron conversion in nuclei like aluminum, titanium and gold is studied in the context of a class of mirror fermion model with non-sterile right-handed neutrinos having mass at the electroweak scale. At the limit of zero momentum transfer and large mirror lepton masses, we derive a simple formula to relate the conversion rate with the on-shell radiative decay rate of muon into electron. Current experimental limits (SINDRUM II) and projected sensitivities (Mu2e, COMET and PRISM) for the muon-to-electron conversion rates in various nuclei and latest limit from MEG for the radiative decay rate of muon into electron are used to put constraints on the parameter space of the model. Depending on the nuclei targets used in different experiments, for the mirror lepton mass in the range of 100 to 800 GeV, the sensitivities of the new Yukawa couplings one can probe in the near future are in the range of one tenth to one hundred-thousandth, depending on the mixing scenarios in the model.

I. INTRODUCTION

As is well known, lepton flavor is an accidental conserved quantity in Standard Model (SM) with strictly massless neutrinos. For example, a muon never decays radiatively into an electron plus a photon and neutrinos do not oscillate in SM. However various experiments have now established firmly that neutrinos do oscillate from one flavor to another. The common wisdom, motivated by the physics of $K - \bar{K}$ oscillation in the kaon system, is to give tiny masses with small mass differences to the various light neutrino species. Radiative decay of the muon into electron is then possible but with an unobservable rate highly suppressed with the minuscule neutrino masses [1, 2]. Searches for lepton flavor violating rare processes in high intensity experiments are thus important for new physics beyond the SM.

The most updated limit on $B(\mu \rightarrow e\gamma)$ is from MEG experiment [3]

$$B(\mu \rightarrow e\gamma) \leq 4.2 \times 10^{-13} \text{ (90\% C.L.) (MEG 2016)}, \quad (1)$$

and its projected improvement [4] is

$$B(\mu \rightarrow e\gamma) \sim 4 \times 10^{-14}. \quad (2)$$

Recent data from T2K experiment [5] agrees well with the global analysis of neutrino oscillation data [6–8], suggesting that the normal neutrino mass hierarchy (NH) with a CP violating Dirac phase $\delta_{\text{CP}} \sim 3\pi/2$ is slightly preferred. The best fit result for the central values of the PMNS matrix elements in the normal neutrino mass hierarchy can be extracted from [6]

$$U_{\text{PMNS}}^{\text{NH}} = \begin{pmatrix} 0.8251 & 0.5453 & 0.08679 + 0.1195i \\ -0.4568 + 0.0670i & 0.5854 + 0.04428i & 0.6649 \\ 0.3171 + 0.07377i & -0.5963 + 0.04875i & 0.7322 \end{pmatrix}. \quad (3)$$

For the $\mu - e$ conversion in nuclei, the present experimental upper limits on the branching ratios were obtained by SINDRUM II experiment [9, 10] for the targets titanium and gold,

$$B(\mu^- + \text{Ti} \rightarrow e^- + \text{Ti}) < 4.3 \times 10^{-12} \text{ (90\% C.L.)}, \quad (4)$$

$$B(\mu^- + \text{Au} \rightarrow e^- + \text{Au}) < 7 \times 10^{-13} \text{ (90\% C.L.)}. \quad (5)$$

Significant improvements are expected for $\mu - e$ conversion at future experiments like Mu2e at Fermilab in US and COMET at J-PARC in Japan. Projected sensitivities of $\mu - e$ conversion are [11–15]

$$B(\mu^- + \text{Al} \rightarrow e^- + \text{Al}) < 3 \times 10^{-17} \text{ (Mu2e, COMET)}, \quad (6)$$

$$B(\mu^- + \text{Ti} \rightarrow e^- + \text{Ti}) < 10^{-18} \text{ (Mu2e II, PRISM)}. \quad (7)$$

A positive signal of any of the above processes (or any process with charged lepton flavor violation (CLFV)) at the current or projected sensitivities of various high intensity experiments would be a clear indication of new physics as well, just like neutrino oscillations. Given the fact that no new physics has showed up yet at the high energy frontier of the Large Hadron Collider (LHC), it is not a surprise that many recent works have been focused on new physics implication of CLFV in the high intensity frontier. For a review on this topics and its possible connection with the muon anomaly, see [16] and references therein.

In a recent work [17], we updated a previous calculation [18] for the radiative process $\mu \rightarrow e\gamma$ in the mirror fermion model with electroweak scale non-sterile right-handed neutrinos [19] to an extended version [20] where a horizontal A_4 symmetry in the lepton sector was imposed. In this work we extend this previous analysis [17] to the $\mu - e$ conversion in nuclei, in particular for aluminum, gold and titanium.

This paper is organized as follows. In Sec. II, after presenting some highlights of the crucial features of the extended mirror fermion model, the calculation of $\mu - e$

conversion in the model is presented. In Sec. III, we derive a simple relation between the $\mu - e$ conversion rate and the radiative decay rate of $\mu \rightarrow e\gamma$ in the limit of zero momentum transfer and large mirror lepton masses. Numerical results are shown in Sec. IV. We summarize In Sec. V. In Appendix A, we briefly review the effective Lagrangian [21, 22] for describing $\mu - e$ conversion; and in Appendix B, we collect some useful formulas used in Sec. III.

II. MIRROR FERMION MODEL CALCULATION

In this section, we first provide some highlights for the original mirror fermion model [19] and its A_4 extension [20]. Then we compute the effective coupling constants induced at one loop level in the extended model for the $\mu - e$ conversion.

A. Brief Review of Mirror Fermion Model

1. Motivation

The motivation of introducing mirror fermions in [19] was manifold. First of all, it is aesthetically satisfactory to have parity restoration at a higher energy scale while the maximal parity violating interaction (V-A interaction) in SM can be emerged from spontaneous symmetry breaking. This is one of the main reasons for various left-right symmetric models in the literature [23–26]. Secondly, it is important to study non-perturbative effects in SM by discretizing it on the lattice. However it is well known that putting chiral fermion on the lattice is plagued by fermion doubling - an unavoidable consequence of the no-go theorem proved by Nielsen and Ninomiya [27]. Sophisticated techniques like using Wilson fermion, Ginsparg-Wilson fermion, staggered fermion, or domain wall fermion *etc.*, which by violating at least

one of the assumptions in the no-go theorem to get rid of the unwanted species, are often employed to handle this problem in practice. For new physics model builders, it is attractive to add mirror fermions to the SM which makes the theory becomes vector-like at a higher scale and hence one can avoid the fermion doubling problem if formulating on the lattice. Chiral gauge anomalies will then be cancelled automatically in this class of models. The third motivation is the electroweak scale non-sterile right-handed neutrinos introduced in [19]. For each generation, the right-handed neutrino is introduced together with a right-handed heavy charged fermion partner to form a SM $SU(2)$ doublet. Similarly a left-handed heavy mirror charged lepton will be introduced for each right-handed SM charged lepton. Majorana masses can then be given to these right-handed neutrinos via the vacuum expectation value (VEV) of a Higgs triplet with hypercharge $Y = 2$ with mass at the electroweak scale, rather than the grand unification scale in the usual scheme. Tiny Dirac masses can also be given via small VEVs of Higgs singlets with $Y = 0$. This is the electroweak scale see-saw mechanism in mirror fermion model which is testable at the LHC [28, 29].

The original model in [19] has been shown to be consistent with electroweak precision test data [30] as well as the 125 GeV Higgs data from the LHC with an additional mirror Higgs doublet [31]. In [20], the original model was extended with a horizontal A_4 symmetry imposed in the lepton sector to address various issues of lepton mixings. We briefly review this A_4 extension in the next subsection.

2. Particle Content and Its A_4 Assignments

The particle content of leptons and bosons of the model are shown in Table I. The fields l_{Ri}^M and e_{Li}^M are the mirrors of the SM lepton doublet l_{Li} and singlet e_{Ri} respectively for the i -th generation. For the scalars, Φ_M is the mirror Higgs doublet of Φ introduced in [31]; ξ and $\tilde{\chi}$ are the Georgi-Machacek triplets [32, 33]; and ϕ_{0S}

TABLE I. The lepton and scalar sectors in the extended mirror model together with their assignments under the horizontal A_4 symmetry.

Fields	$l_{Li} = \begin{pmatrix} \nu_L \\ e_L \end{pmatrix}_i$	$l_{Ri}^M = \begin{pmatrix} \nu_R \\ e_R^M \end{pmatrix}_i$	e_{Ri}	e_{Li}^M	ϕ_{0S}	$\vec{\phi}_S = \begin{pmatrix} \phi_{1S} \\ \phi_{2S} \\ \phi_{3S} \end{pmatrix}$	Φ	Φ_M	ξ	$\tilde{\chi}$
$SU(2)$	2	2	1	1	1	1	2	2	3	3
$U(1)_Y$	$-1/2$	$-1/2$	-1	-1	0	0	$1/2$	$1/2$	0	2
A_4	3	3	3	3	1	3	1	1	1	1

and $\vec{\phi}_S$ are singlets introduced in [20]. The A_4 assignments of these particles are listed at the second row in Table I. Note that the scalar $SU(2)$ singlet $\vec{\phi}_S$ is a A_4 triplet with its three components shown explicitly in the Table.

The singlet scalars $\phi_{0S}, \vec{\phi}_S$ are the only fields connecting the SM fermions and their mirror counterparts. Recall that the tetrahedron symmetry group A_4 has four irreducible representations **1**, **1'**, **1''**, and **3** with the following multiplication rule ¹:

$$\begin{aligned} \mathbf{3} \times \mathbf{3} &= \mathbf{3}_1(23, 31, 12) + \mathbf{3}_2(32, 13, 21) \\ &+ \mathbf{1}(11 + 22 + 33) + \mathbf{1}'(11 + \omega^2 22 + \omega 33) + \mathbf{1}''(11 + \omega 22 + \omega^2 33) \end{aligned} \quad (8)$$

where $\omega = e^{2\pi i/3}$. In the gauge eigenbasis (fields with superscript 0), one can write down the following A_4 invariant Yukawa couplings,

$$\begin{aligned} -\mathcal{L}_S &= g_{0S}\phi_{0S}(\bar{l}_L^0 l_R^{0M})_{\mathbf{1}} + g_{1S}\vec{\phi}_S \cdot (\bar{l}_L^0 \times l_R^{0M})_{\mathbf{3}_1} + g_{2S}\vec{\phi}_S \cdot (\bar{l}_L^0 \times l_R^{0M})_{\mathbf{3}_2} + \text{H.c.} \\ &+ g'_{0S}\phi_{0S}(\bar{e}_R^0 e_L^{0M})_{\mathbf{1}} + g'_{1S}\vec{\phi}_S \cdot (\bar{e}_R^0 \times e_L^{0M})_{\mathbf{3}_1} + g'_{2S}\vec{\phi}_S \cdot (\bar{e}_R^0 \times e_L^{0M})_{\mathbf{3}_2} + \text{H.c.} \end{aligned} \quad (9)$$

¹ **3**₁ is differ from **3**₂ because A_4 is nonabelian.

As shown in [20], after the scalar singlets develop VEVs with $v_0 = \langle \phi_{0S} \rangle$ and $v_i = \langle \phi_{iS} \rangle$, one obtains the neutrino mass matrix from the first line of (9)

$$M_\nu^{\text{Dirac}} = \begin{pmatrix} g_{0S}v_0 & g_{1S}v_3 & g_{2S}v_2 \\ g_{2S}v_3 & g_{0S}v_0 & g_{1S}v_1 \\ g_{1S}v_2 & g_{2S}v_1 & g_{0S}v_0 \end{pmatrix}. \quad (10)$$

Hermiticity of the M_ν^{Dirac} implies $g_{2S} = g_{1S}^*$. Furthermore, if one assumes $v_i = v$, M_ν^{Dirac} reduces to

$$M_\nu^{\text{Dirac}} = \begin{pmatrix} g_{0S}v_0 & g_{1S}v & g_{1S}^*v \\ g_{1S}^*v & g_{0S}v_0 & g_{1S}v \\ g_{1S}v & g_{1S}^*v & g_{0S}v_0 \end{pmatrix}. \quad (11)$$

The above form of M_ν^{Dirac} can be diagonalized by unitary transformation, *i.e.* $U_\nu^\dagger M_\nu^{\text{Dirac}} U_\nu = M_\nu^{\text{Diag}}$ with

$$U_\nu \equiv U_{\text{CW}} = \frac{1}{\sqrt{3}} \begin{pmatrix} 1 & 1 & 1 \\ 1 & \omega^2 & \omega \\ 1 & \omega & \omega^2 \end{pmatrix}, \quad (12)$$

where ω is the same as in the multiplication rules of A_4 given in (8). The matrix U_{CW} in (12) was first discussed by Cabibbo [34] and also by Wolfenstein [35] in the context of CP violation in three generations of neutrino oscillations. In recent years, advocating A_4 symmetry in the lepton sector was mainly due to Ma [36].

TABLE II. Matrix elements for the four auxiliary $M^k (k = 0, 1, 2, 3)$ where $\omega \equiv \exp(i2\pi/3)$ and g_{0S} and g_{1S} are complex Yukawa couplings. M'^k can be obtained from M^k with the following substitutions $g_{0S} \rightarrow g'_{0S}$ and $g_{1S} \rightarrow g'_{1S}$.

M_{jn}^k	Value
$M_{12}^0, M_{13}^0, M_{21}^0, M_{23}^0, M_{31}^0, M_{32}^0$	0
$M_{11}^0, M_{22}^0, M_{33}^0$	g_{0S}
$M_{11}^1, M_{11}^2, M_{11}^3; M_{23}^1, M_{32}^1$	$\frac{2}{3}\text{Re}(g_{1S})$
$M_{22}^1, M_{22}^2, M_{22}^3; M_{13}^1, M_{31}^1$	$\frac{2}{3}\text{Re}(\omega^* g_{1S})$
$M_{33}^1, M_{33}^2, M_{33}^3; M_{12}^1, M_{21}^1$	$\frac{2}{3}\text{Re}(\omega g_{1S})$
M_{12}^2, M_{21}^3	$\frac{1}{3}(g_{1S} + \omega g_{1S}^*)$
M_{12}^3, M_{21}^2	$\frac{1}{3}(g_{1S}^* + \omega^* g_{1S})$
M_{13}^2, M_{31}^3	$\frac{1}{3}(g_{1S} + \omega^* g_{1S}^*)$
M_{13}^3, M_{31}^2	$\frac{1}{3}(g_{1S}^* + \omega g_{1S})$
M_{23}^2, M_{32}^3	$\frac{2\omega^*}{3}\text{Re}(g_{1S})$
M_{23}^3, M_{32}^2	$\frac{2\omega}{3}\text{Re}(g_{1S})$

3. Mixings

Let $U_{L,R}^l$ and $U_{R,L}^{l^M}$ be the unitary matrices relating the gauge eigenstates and the mass eigenstates (fields without superscripts 0) defined as

$$l_L^0 = U_L^l l_L, \quad e_R^0 = U_R^l e_R, \quad l_R^{M,0} = U_R^{l^M} l_R^M, \quad e_L^{M,0} = U_L^{l^M} e_L^M. \quad (13)$$

Following [17], we express the Yukawa couplings in (9) as follows

$$\mathcal{L}_S^l = - \sum_{k=0}^3 \sum_{i,m=1}^3 \left(\bar{l}_{Li} \mathcal{U}_{im}^{Lk} l_{Rm}^M + \bar{e}_{Ri} \mathcal{U}_{im}^{Rk} e_{Lm}^M \right) \phi_{kS} + \text{H.c.} \quad (14)$$

The coupling coefficients \mathcal{U}_{im}^{Lk} and \mathcal{U}_{im}^{Rk} are given by

$$\begin{aligned}\mathcal{U}_{im}^{Lk} &\equiv \left(U_{\text{PMNS}}^\dagger \cdot M^k \cdot U_{\text{PMNS}}^M \right)_{im} , \\ &= \sum_{j,n=1}^3 \left(U_{\text{PMNS}}^\dagger \right)_{ij} M_{jn}^k (U_{\text{PMNS}}^M)_{nm} ,\end{aligned}\tag{15}$$

$$\begin{aligned}\mathcal{U}_{im}^{Rk} &\equiv \left(U_{\text{PMNS}}'^\dagger \cdot M'^k \cdot U_{\text{PMNS}}'^M \right)_{im} , \\ &= \sum_{j,n=1}^3 \left(U_{\text{PMNS}}'^\dagger \right)_{ij} M_{jn}'^k (U_{\text{PMNS}}'^M)_{nm} ,\end{aligned}\tag{16}$$

where the matrix elements for the four auxiliary matrices $M^k (k = 0, 1, 2, 3)$ are listed in Table II, and $M_{jn}'^k$ can be obtained from M_{jn}^k with the following substitutions for the Yukawa couplings $g_{0S} \rightarrow g_{0S}'$ and $g_{1S} \rightarrow g_{1S}'$; U_{PMNS} is the usual neutrino mixing matrix defined as

$$U_{\text{PMNS}} = U_\nu^\dagger U_L^l ,\tag{17}$$

and its mirror and right-handed counter-parts U_{PMNS}^M , U_{PMNS}' and $U_{\text{PMNS}}'^M$ are defined analogously as

$$U_{\text{PMNS}}^M = U_\nu^\dagger U_R^{lM} ,\tag{18}$$

$$U_{\text{PMNS}}' = U_\nu^\dagger U_R^l ,\tag{19}$$

and

$$U_{\text{PMNS}}'^M = U_\nu^\dagger U_L^{lM} .\tag{20}$$

B. Photon Contributions and the Monopole and Dipole Form Factors

In this work we will focus on the contributions from the photon exchange as shown in the Feynman Diagrams of Fig. 1. We also compute the contributions from the Z-exchange but since they are suppressed by m_μ^2/m_Z^2 we will not present them here.

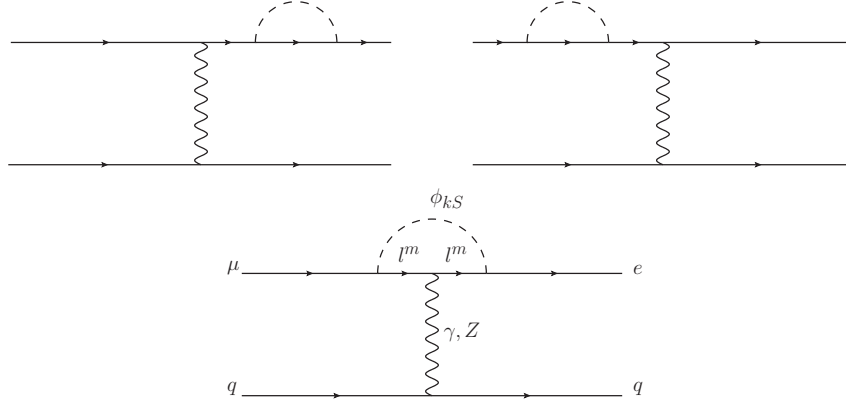


FIG. 1. One-loop induced Feynman diagrams from photon and Z boson exchanges for $\mu - e$ conversion in electroweak-scale ν_R model.

The invariant amplitude for $\mu^-(p) \rightarrow e^-(p')\gamma^*(q)$ with an off-shell photon can be parametrized as

$$i\mathcal{M}_\gamma = -e\bar{u}_e(p')i\Gamma_\gamma^\mu(q)u_\mu(p)A_\mu^*(q) \quad (21)$$

where $\Gamma_\gamma^\mu(q)$ has the following Lorentz and gauge invariant decomposition

$$\Gamma_\gamma^\mu(q) = (f_{E0}(q^2) + \gamma_5 f_{M0}(q^2)) \left(\gamma^\mu - \frac{q_\mu \not{q}}{q^2} \right) + (f_{M1}(q^2) + \gamma_5 f_{E1}(q^2)) \frac{i\sigma^{\mu\nu} q_\nu}{m_\mu}. \quad (22)$$

The monopole form factors f_{E0} , f_{M0} and the dipole form factors f_{M1} , f_{E1} can be obtained by generalizing our previous on-shell calculation of $\mu \rightarrow e\gamma$ in the same model [17] to the case of off-shell photon γ^* . From the Feynman diagrams of Fig. 1,

we obtain the following expressions

$$\begin{aligned}
f_{E0,M0}(q^2) = & + \frac{1}{32\pi^2} \sum_{k,m} \int_0^1 dx \int_0^{1-x} dy \left\{ \frac{xyq^2}{\Delta_{km}(q^2)} \left(\mathcal{U}_{1m}^{Lk} (\mathcal{U}_{2m}^{Lk})^* \pm \mathcal{U}_{1m}^{Rk} (\mathcal{U}_{2m}^{Rk})^* \right) \right. \\
& - \left[\log \left(\frac{\Delta_{km}(q^2)}{\Delta_{km}(0)} \right) - (M_m^2 \pm (1-x-y)^2 m_\mu m_e) (\Delta_{km}^{-1}(q^2) - \Delta_{km}^{-1}(0)) \right] \\
& \times \left(\mathcal{U}_{1m}^{Lk} (\mathcal{U}_{2m}^{Lk})^* \pm \mathcal{U}_{1m}^{Rk} (\mathcal{U}_{2m}^{Rk})^* \right) \\
& + (1-x-y)(m_\mu \pm m_e) M_m (\Delta_{km}^{-1}(q^2) - \Delta_{km}^{-1}(0)) \\
& \left. \times \left(\mathcal{U}_{1m}^{Lk} (\mathcal{U}_{2m}^{Rk})^* \pm \mathcal{U}_{1m}^{Rk} (\mathcal{U}_{2m}^{Lk})^* \right) \right\} \quad (23)
\end{aligned}$$

for the monopole form factors, and

$$\begin{aligned}
f_{M1,E1}(q^2) = & - \frac{m_\mu}{32\pi^2} \sum_{k,m} \int_0^1 dx \int_0^{1-x} dy \frac{1}{\Delta_{km}(q^2)} \\
& \times \left\{ (1-x-y)(ym_\mu \pm xm_e) \left(\mathcal{U}_{1m}^{Lk} (\mathcal{U}_{2m}^{Lk})^* \pm \mathcal{U}_{1m}^{Rk} (\mathcal{U}_{2m}^{Rk})^* \right) \right. \\
& \left. + (x+y) M_m \left(\mathcal{U}_{1m}^{Lk} (\mathcal{U}_{2m}^{Rk})^* \pm \mathcal{U}_{1m}^{Rk} (\mathcal{U}_{2m}^{Lk})^* \right) \right\} \quad (24)
\end{aligned}$$

for the dipole form factors. Here, we have defined

$$\Delta_{km}(q^2) = (x+y)M_m^2 + (1-x-y)(m_k^2 - xm_e^2 - ym_\mu^2) - xyq^2 - i0^+, \quad (25)$$

where m_k denotes the mass of scalar singlet ϕ_{kS} for $k = 0, 1, 2, 3$ and M_m the mass of mirror lepton l_m^M for $m = 1, 2, 3$.

At $q^2 = 0$, we have $f_{E0,M0}(0) = 0$ as one would expect. Thus the following reduced monopole form factors $\tilde{f}_{E0,M0}$ with an explicit factor of q^2 extracted from $f_{E0,M0}$ are often defined in the literature,

$$f_{E0,M0}(q^2) = \frac{q^2}{m_\mu^2} \tilde{f}_{E0,M0}(q^2). \quad (26)$$

For small q^2 , one can set $\tilde{f}_{E0,M0}(q^2) \approx \tilde{f}_{E0,M0}(0)$ with

$$\begin{aligned} \tilde{f}_{E0,M0}(0) = & \frac{m_\mu^2}{32\pi^2} \sum_{k,m} \int_0^1 dx \int_0^{1-x} dy \frac{xy}{(\Delta_{km}(0))^2} \left\{ \left(\mathcal{U}_{1m}^{Lk} (\mathcal{U}_{2m}^{Lk})^* \pm \mathcal{U}_{1m}^{Rk} (\mathcal{U}_{2m}^{Rk})^* \right) \right. \\ & \times \left(2\Delta_{km}(0) + M_m^2 \pm (1-x-y)^2 m_\mu m_e \right) \\ & \left. + \left(\mathcal{U}_{1m}^{Lk} (\mathcal{U}_{2m}^{Rk})^* \pm \mathcal{U}_{1m}^{Rk} (\mathcal{U}_{2m}^{Lk})^* \right) (1-x-y)(m_\mu \pm m_e) M_m \right\}. \end{aligned} \quad (27)$$

The explicit factor of q^2 in (26) will cancel the $1/q^2$ of the photon propagator in Fig. 1. This leads to four-fermion vector-vector interaction and hence the reduced monopole form factors will contribute to the effective coupling $C_{V(R,L)}^{(q)}$ in the effective Lagrangian of (48) in Appendix A. We will discuss more about these four-fermion interactions in the next subsection.

At $q^2 = 0$, the contributions from the magnetic and electric dipole terms of (22) to the amplitude \mathcal{M}_γ in (21) can be reproduced by the following effective Lagrangian

$$\mathcal{L}_{\gamma,\text{eff}} = \frac{e}{2m_\mu} \bar{e} \sigma^{\alpha\beta} (f_{M1}(0) + \gamma_5 f_{E1}(0)) \mu F_{\alpha\beta} + \text{H.c.} . \quad (28)$$

Comparing (28) with the first line of the general form of the Lagrangian for $\mu - e$ conversion given in (48) in Appendix A, one can deduce the dimensionless effective couplings $C_{DR,DL}$ as linear combinations of the static limit of the dipole form factors f_{E1} and f_{M1} ,

$$\frac{C_{DR,DL}}{\Lambda^2} = \frac{e}{2m_\mu^2} (\pm f_{E1}(0) - f_{M1}(0)) . \quad (29)$$

C. Four-Fermion Coupling Constants $C_{V(L,R)}^{(q)}$ - Photon Exchange

The amplitude for $\mu(p)q(k) \rightarrow e(p')q(k')$ from the monopole form factors of the photon exchange in Fig. 1 can be obtained as

$$\mathcal{M}_\gamma = -e^2 Q_q \bar{u}_e(p') (f_{E0}(q^2) + f_{M0}(q^2) \gamma_5) \left(\gamma_\mu - \frac{q_\mu \not{q}}{q^2} \right) u_\mu(p) \frac{1}{q^2} \bar{u}_q(k') \gamma^\mu u_q(k) , \quad (30)$$

where $q = p - p' = k' - k$, and f_{E0} , f_{M0} are given in (23). The q_μ term in (30) can be dropped due to quark current conservation. As mentioned earlier, the $1/q^2$ of the photon propagator will be cancelled from a factor of q^2 in $f_{E0,M0}$. Thus in terms of the reduced form factors $\tilde{f}_{E0,M0}$ of (26), the amplitude \mathcal{M}_γ can be rewritten as

$$\mathcal{M}_\gamma = -\frac{e^2 Q_q}{m_\mu^2} \left[\left(\tilde{f}_{E0} - \tilde{f}_{M0} \right) \overline{u}_{Le}(p') \gamma_\mu u_{L\mu}(p) + \left(\tilde{f}_{E0} + \tilde{f}_{M0} \right) \overline{u}_{Re}(p') \gamma_\mu u_{R\mu}(p) \right] \\ \times [\overline{u}_{Lq}(k') \gamma^\mu u_{Lq}(k) + \overline{u}_{Rq}(k') \gamma^\mu u_{Rq}(k)] , \quad (31)$$

where $\tilde{f}_{E0,M0}$ are defined in (27) for small q^2 . At $q^2 = 0$, this amplitude can be reproduced by the following Fermi interaction

$$\mathcal{L}'_{\gamma,\text{eff}} = -\frac{e^2 Q_q}{m_\mu^2} \left[\left(\tilde{f}_{E0}(0) - \tilde{f}_{M0}(0) \right) \overline{e}_L \gamma_\mu \mu_L + \left(\tilde{f}_{E0}(0) + \tilde{f}_{M0}(0) \right) \overline{e}_R \gamma_\mu \mu_R \right] \\ \times [\overline{q} \gamma^\mu q] . \quad (32)$$

By matching (32) with the second line of the general form of the Lagrangian for $\mu - e$ conversion given in (48) in Appendix A, we deduce the following relations for the dimensionless effective couplings $C_{V(L,R)}^{(q)\gamma}$

$$\frac{C_{V(L,R)}^{(q)\gamma}}{\Lambda^2} = \frac{e^2 Q_q}{m_\mu^2} \left(\tilde{f}_{E0}(0) \mp \tilde{f}_{M0}(0) \right) . \quad (33)$$

Note that we have the relation $C_{V(L,R)}^{(u)\gamma} = -2C_{V(L,R)}^{(d)\gamma}$. This implies the vector effective couplings $\tilde{C}_{V(L,R)}^{(n)\gamma}$ for the neutron from the photon exchange are vanishing. This is expected since neutron carries no electric charge.

We also note that for the photon contributions, only $C_{VR}^{(q)}$ and $C_{VL}^{(q)}$ are non-vanishing. Other four-fermion effective couplings will be non-vanishing only from Z exchange, scalar exchange or box diagrams, which are negligible as compared with the photon exchange contributions.

III. THE RELATIONSHIP BETWEEN $\mu - e$ CONVERSION AND $\mu \rightarrow e\gamma$

Since the momentum transfer q^2 is expected to be quite small in the $\mu - e$ conversion process in nuclei, we can make a Taylor expansion for the various form factors deduced in the previous section around $q^2 = 0$. Thus for small q^2 , we have

$$f_{E0,M0}(q^2) \approx \frac{q^2}{32\pi^2} \frac{1}{M_m^4} \sum_{k,m} \left\{ \left(\mathcal{U}_{1m}^{Lk} (\mathcal{U}_{2m}^{Lk})^* \pm \mathcal{U}_{1m}^{Rk} (\mathcal{U}_{2m}^{Rk})^* \right) \times \left[M_m^2 (\mathcal{I}(r_{km}) + 2\mathcal{I}_{30}(r_{km})) \pm m_\mu m_e \mathcal{I}_{10}(r_{km}) \right] \right. \\ \left. + \left(\mathcal{U}_{1m}^{Lk} (\mathcal{U}_{2m}^{Rk})^* \pm \mathcal{U}_{1m}^{Rk} (\mathcal{U}_{2m}^{Lk})^* \right) M_m (m_\mu \pm m_e) \mathcal{I}_{20}(r_{km}) \right\}, \quad (34)$$

and

$$f_{M1,E1}(q^2) \approx - \frac{m_\mu}{32\pi^2} \sum_{k,m} \left\{ \frac{1}{M_m^2} (m_\mu \pm m_e) \left(\mathcal{U}_{1m}^{Lk} (\mathcal{U}_{2m}^{Lk})^* \pm \mathcal{U}_{1m}^{Rk} (\mathcal{U}_{2m}^{Rk})^* \right) \mathcal{I}(r_{km}) \right. \\ \left. + \frac{1}{M_m} \left(\mathcal{U}_{1m}^{Lk} (\mathcal{U}_{2m}^{Rk})^* \pm \mathcal{U}_{1m}^{Rk} (\mathcal{U}_{2m}^{Lk})^* \right) \mathcal{J}(r_{km}) \right\} \\ - \frac{m_\mu q^2}{32\pi^2} \left\{ \frac{1}{M_m^4} (m_\mu \pm m_e) \left(\mathcal{U}_{1m}^{Lk} (\mathcal{U}_{2m}^{Lk})^* \pm \mathcal{U}_{1m}^{Rk} (\mathcal{U}_{2m}^{Rk})^* \right) \mathcal{I}_{40}(r_{km}) \right. \\ \left. + \frac{1}{M_m^3} \left(\mathcal{U}_{1m}^{Lk} (\mathcal{U}_{2m}^{Rk})^* \pm \mathcal{U}_{1m}^{Rk} (\mathcal{U}_{2m}^{Lk})^* \right) \mathcal{I}_{50}(r_{km}) \right\}. \quad (35)$$

Here $r_{km} = m_k^2/M_m^2$ and the expressions for the Feynman parameterization integrals \mathcal{I} , \mathcal{J} and \mathcal{I}_{i0} ($i = 1, 2, \dots, 5$) can be found in Appendix B.

From (49) in Appendix B, the conversion rate (for γ exchange) is given by

$$\Gamma_{\text{conv}} = \frac{m_\mu^5}{4\Lambda^4} \left(\left| C_{DR} D + 4\tilde{C}_{VR}^{(p)} V^{(p)} \right|^2 + \left| C_{DL} D + 4\tilde{C}_{VL}^{(p)} V^{(p)} \right|^2 \right), \quad (36)$$

where $C_{DR,DL}$ is given by (29), and $\tilde{C}_{VR,VL}^{(p)}$ are given by (50) and (52) in Appendix A. To obtain (36), we have used the following result valid for the neutron,

$$\tilde{C}_{V(L,R)}^{(n)} = \sum_{u,d,s} C_{V(L,R)}^{(q)} f_{Vn}^{(q)} = 0. \quad (37)$$

Using the above approximate form factors (34) and (35) for small q^2 , we can derive

$$\begin{aligned}
C_{DR,DL} \approx \frac{e\Lambda^2}{32\pi^2 m_\mu} \sum_{k,m} \Bigg\{ & \frac{\mathcal{I}(r_{km})}{M_m^2} \left(m_\mu \mathcal{U}_{1m}^{R,Lk} \left(\mathcal{U}_{2m}^{R,Lk} \right)^* + m_e \mathcal{U}_{1m}^{L,Rk} \left(\mathcal{U}_{2m}^{L,Rk} \right)^* \right) \\
& + \frac{\mathcal{J}(r_{km})}{M_m} \mathcal{U}_{1m}^{R,Lk} \left(\mathcal{U}_{2m}^{L,Rk} \right)^* \\
& + \frac{q^2}{M_m^2} \left[\frac{\mathcal{I}_{40}(r_{km})}{M_m^2} \left(m_\mu \mathcal{U}_{1m}^{R,Lk} \left(\mathcal{U}_{2m}^{R,Lk} \right)^* + m_e \mathcal{U}_{1m}^{L,Rk} \left(\mathcal{U}_{2m}^{L,Rk} \right)^* \right) \right. \\
& \left. + \frac{\mathcal{I}_{50}(r_{km})}{M_m} \mathcal{U}_{1m}^{R,Lk} \left(\mathcal{U}_{2m}^{L,Rk} \right)^* \right] \Bigg\}, \quad (38)
\end{aligned}$$

and summing over the contributions from light quarks, we have

$$\begin{aligned}
\tilde{C}_{VL,VR}^{(p)} \approx \frac{e^2 \Lambda^2}{16\pi^2 M_m^4} \sum_{k,m} \Bigg\{ & M_m^2 (\mathcal{I}(r_{km}) + 2 \mathcal{I}_{30}(r_{km})) \mathcal{U}_{1m}^{R,Lk} \left(\mathcal{U}_{2m}^{R,Lk} \right)^* \\
& + m_\mu m_e \mathcal{I}_{10}(r_{km}) \mathcal{U}_{1m}^{L,Rk} \left(\mathcal{U}_{2m}^{L,Rk} \right)^* \\
& + M_m \mathcal{I}_{20}(r_{km}) \left(m_\mu \mathcal{U}_{1m}^{R,Lk} \left(\mathcal{U}_{2m}^{L,Rk} \right)^* + m_e \mathcal{U}_{1m}^{L,Rk} \left(\mathcal{U}_{2m}^{R,Lk} \right)^* \right) \Bigg\}. \quad (39)
\end{aligned}$$

Dropping the q^2 terms in $C_{DR,DL}$ and keeping only those terms up to $\mathcal{O}(1/M_m^2)$ in $\tilde{C}_{VL,VR}^{(p)}$, we obtain for the conversion rate

$$\begin{aligned}
\Gamma_{\text{conv}}(q^2 \rightarrow 0) \approx & \frac{m_\mu^5}{4} \frac{1}{(32\pi^2)^2} \\
& \times \sum_{k,m} \Bigg\{ \left| \frac{16\pi^2 D}{m_\mu} C_L^{km} + 8V^{(p)} e^2 \frac{\mathcal{I}(r_{km}) + 2 \mathcal{I}_{30}(r_{km})}{M_m^2} \mathcal{U}_{1m}^{Lk} \left(\mathcal{U}_{2m}^{Lk} \right)^* \right|^2 \\
& + \left| \frac{16\pi^2 D}{m_\mu} C_R^{km} + 8V^{(p)} e^2 \frac{\mathcal{I}(r_{km}) + 2 \mathcal{I}_{30}(r_{km})}{M_m^2} \mathcal{U}_{1m}^{Rk} \left(\mathcal{U}_{2m}^{Rk} \right)^* \right|^2 \Bigg\} \quad (40)
\end{aligned}$$

where

$$\begin{aligned}
C_{L,R}^{km} = \frac{e}{16\pi^2} \Bigg\{ & \frac{\mathcal{I}(r_{km})}{M_m^2} \left(m_\mu \mathcal{U}_{1m}^{R,Lk} \left(\mathcal{U}_{2m}^{R,Lk} \right)^* + m_e \mathcal{U}_{1m}^{L,Rk} \left(\mathcal{U}_{2m}^{L,Rk} \right)^* \right) \\
& + \frac{\mathcal{J}(r_{km})}{M_m} \mathcal{U}_{1m}^{R,Lk} \left(\mathcal{U}_{2m}^{L,Rk} \right)^* \Bigg\}. \quad (41)
\end{aligned}$$

Recall that for the on-shell process $\mu \rightarrow e\gamma$, we have

$$\Gamma_{\mu \rightarrow e\gamma} = \frac{1}{16\pi} m_\mu^3 \sum_{k,m} (|C_L^{km}|^2 + |C_R^{km}|^2) . \quad (42)$$

Thus, one obtains

$$\begin{aligned} \Gamma_{\text{conv}}(q^2 \rightarrow 0) \approx \pi D^2 \Gamma_{\mu \rightarrow e\gamma} + \frac{m_\mu^5}{(64\pi^2)^2} \sum_{k,m} & \left\{ 2DV^{(p)} (8\pi e)^2 \frac{\mathcal{I}(r_{km}) + 2\mathcal{I}_{30}(r_{km})}{m_\mu M_m^2} \right. \\ & \times \left(C_L^{km} \mathcal{U}_{1m}^{Lk} (\mathcal{U}_{2m}^{Lk})^* + (C_L^{km})^* (\mathcal{U}_{1m}^{Lk})^* \mathcal{U}_{2m}^{Lk} \right. \\ & \quad \left. + C_R^{km} \mathcal{U}_{1m}^{Rk} (\mathcal{U}_{2m}^{Rk})^* + (C_R^{km})^* (\mathcal{U}_{1m}^{Rk})^* \mathcal{U}_{2m}^{Rk} \right) \\ & \left. + \left(8V^{(p)} e^2 \frac{\mathcal{I}(r_{km}) + 2\mathcal{I}_{30}(r_{km})}{M_m^2} \right)^2 \left(|\mathcal{U}_{1m}^{Lk} (\mathcal{U}_{2m}^{Lk})^*|^2 + |\mathcal{U}_{1m}^{Rk} (\mathcal{U}_{2m}^{Rk})^*|^2 \right) \right\} . \end{aligned} \quad (43)$$

Note that since $C_{L,R}^{km}$ is scaled by $1/M_m$, the second and the third terms in (43) are suppressed by $1/M_m$ and $1/M_m^2$ respectively, as compared with the first term. If one drops these two suppressed terms further, one obtains a simple relation

$$\Gamma_{\text{conv}}(q^2 \rightarrow 0) \approx \pi D^2 \Gamma_{\mu \rightarrow e\gamma} . \quad (44)$$

Thus,

$$B_{\mu N \rightarrow e N} = \frac{\Gamma_{\text{conv}}}{\Gamma_{\text{capt}}} \approx \pi D^2 \frac{\Gamma_\mu}{\Gamma_{\text{capt}}} B_{\mu \rightarrow e\gamma} , \quad (45)$$

where Γ_μ is the total decay width of the muon.

IV. NUMERICAL ANALYSIS

In our analysis, we adapt the same assumptions for the parameter space as was done in [17]. We summarize them as follows.

- For the mass parameters, we take the masses of the singlet scalars ϕ_{kS} to be

$$m_0 : m_1 : m_2 : m_3 = M_S : 2M_S : 3M_S : 4M_S , \quad (46)$$

where the common mass M_S is set to be 10 MeV; and for the mirror lepton masses, we set

$$M_m = M_{\text{mirror}} + \delta_m \quad (47)$$

where $\delta_1 = 0$, $\delta_2 = 10$ GeV, $\delta_3 = 20$ GeV and the common mass M_{mirror} is varied in the range of 100 – 800 GeV. Our results are insensitive to these choices as long as $m_k/M_m \ll 1$.

- Note that the relations $g_{2S} = (g_{1S})^*$ and $g'_{2S} = (g'_{1S})^*$ hold due to the hermiticity of the neutrino Dirac mass matrix. However, all the Yukawa couplings g_{0S} , g_{1S} , g_{2S} , g'_{0S} , g'_{1S} , and g'_{2S} are assumed to be real.
- Out of the four mixing matrices, only the one U_{PMNS} associated with the left-handed SM fermions are known. Following [17], we will consider two scenarios below:

- Scenario 1: $U_{\text{PMNS}}^M = U'_{\text{PMNS}} = U'^M_{\text{PMNS}} = U_{\text{CW}}^\dagger$
- Scenario 2: $U_{\text{PMNS}}^M = U'_{\text{PMNS}} = U'^M_{\text{PMNS}} = U_{\text{PMNS}}$

where U_{CW} is given by (12). For the PMNS mixing matrix, we will use the best fit result in (3). In the two scenarios that we are studying, our results do not depend sensitively on the mass hierarchies.

- We will study the following two cases for the Yukawa couplings.
 1. $g_{0S} = g'_{0S}$ and $g_{1S} = g'_{1S} = 10^{-2}g_{0S}$. Hence the contributions from the A_4 triplet is small.
 2. $g_{0S} = g'_{0S} = g_{1S} = g'_{1S}$. Both A_4 singlet and triplet terms carry the same weight.

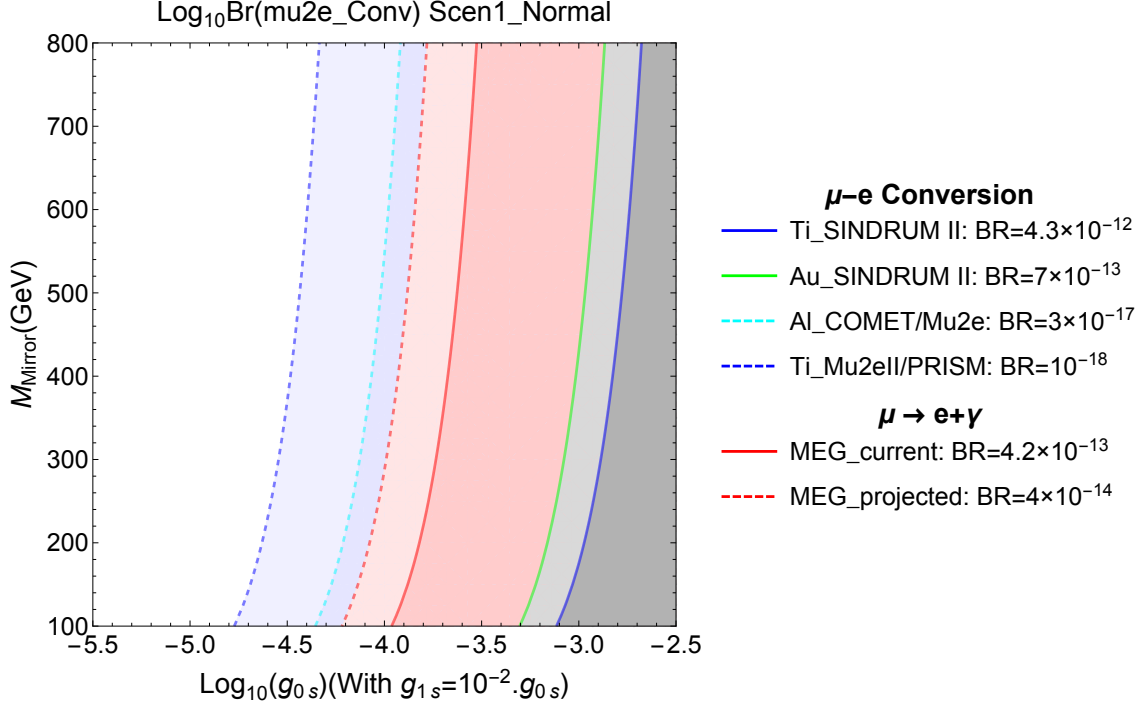


FIG. 2. Contour plots of $\text{Log}_{10} B(\mu - e \text{ conversion})$ on the $(g_{0S}, M_{\text{mirror}})$ plane for normal mass hierarchy in Scenario 1 with $g_{0S} = g'_{0S}$ and $g_{1S} = g'_{1S} = 10^{-2} g_{0S}$. The legend shows current experimental limits and projected sensitivities from COMET, Mu2e, SINDRUM II, PRISM and MEG. For details of other input parameters, one can refer to the text in Sec. IV.

In Figs. 2, 3, 4 and 5 we plot the contour of $\log_{10} B(\mu - e \text{ conversion})$ with γ dominance in the $(\log_{10}(g_{0S}), M_{\text{mirror}})$ plane for Scenarios 1 and 2 with the normal neutrino mass hierarchy for the 2 cases of couplings aforementioned respectively. The blue and green solid lines correspond to the current limits from SINDRUM II experiments for $\mu - e$ conversion to titanium (4) and gold (5) respectively. The red solid and dashed lines correspond to the current limit (1) and projected sensitivity (2) for $\mu \rightarrow e\gamma$ from MEG experiment. The cyan and blue dashed lines correspond to the

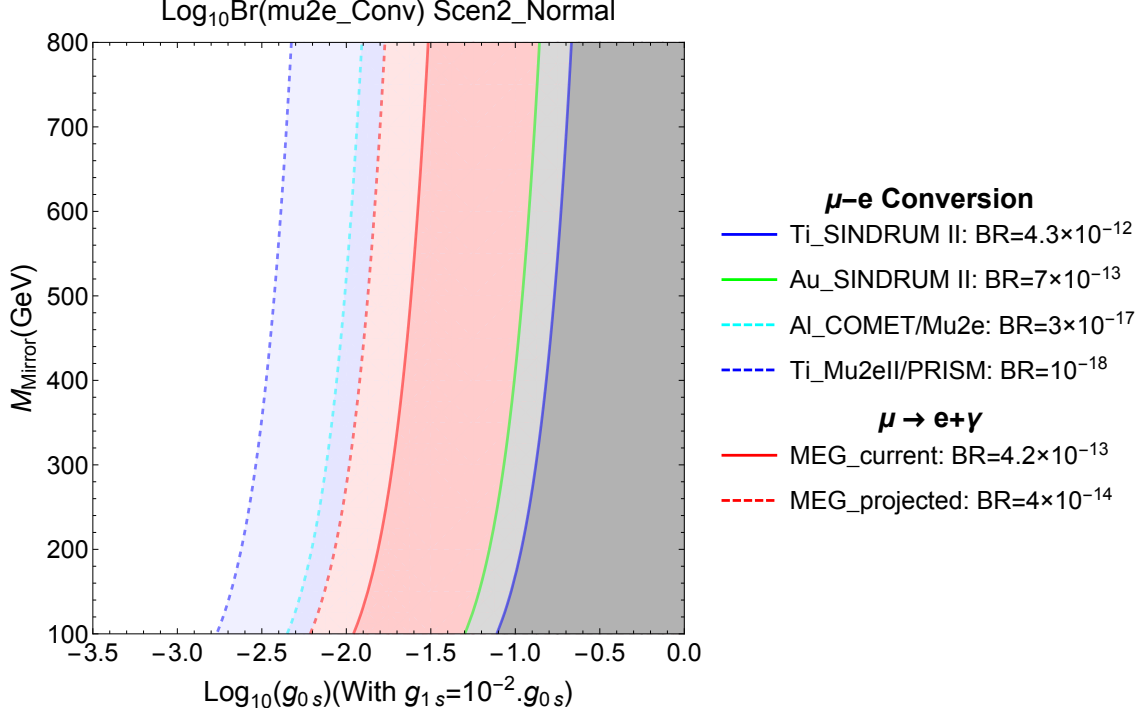


FIG. 3. Contour plots of $\text{Log}_{10} B(\mu - e \text{ conversion})$ on the $(g_{0S}, M_{\text{mirror}})$ plane for normal mass hierarchy in Scenarios 2 with $g_{0S} = g'_{0S}$ and $g_{1S} = g'_{1S} = 10^{-2}g_{0S}$.

projected sensitivities for $\mu - e$ conversion to aluminum and titanium from COMET, Mu2e (6) and Mu2e II, PRISM (7) experiments respectively.

Several comments are in order here.

- We have studied in some details the effects of different settings of couplings on our results. Generally, we observe that as one varies the A_4 triplet coupling g_{1S} from $10^{-2}g_{0S}$ to g_{0S} (from Figs. 2 to 5) the contour plots for $\log_{10} B(\mu - e \text{ conversion})$ are shifted to the left. The A_4 triplet is playing a significant role in putting constraints on the parameter space for the CLFV processes, such as $\mu \rightarrow e\gamma$ and $\mu - e$ conversion in the model.

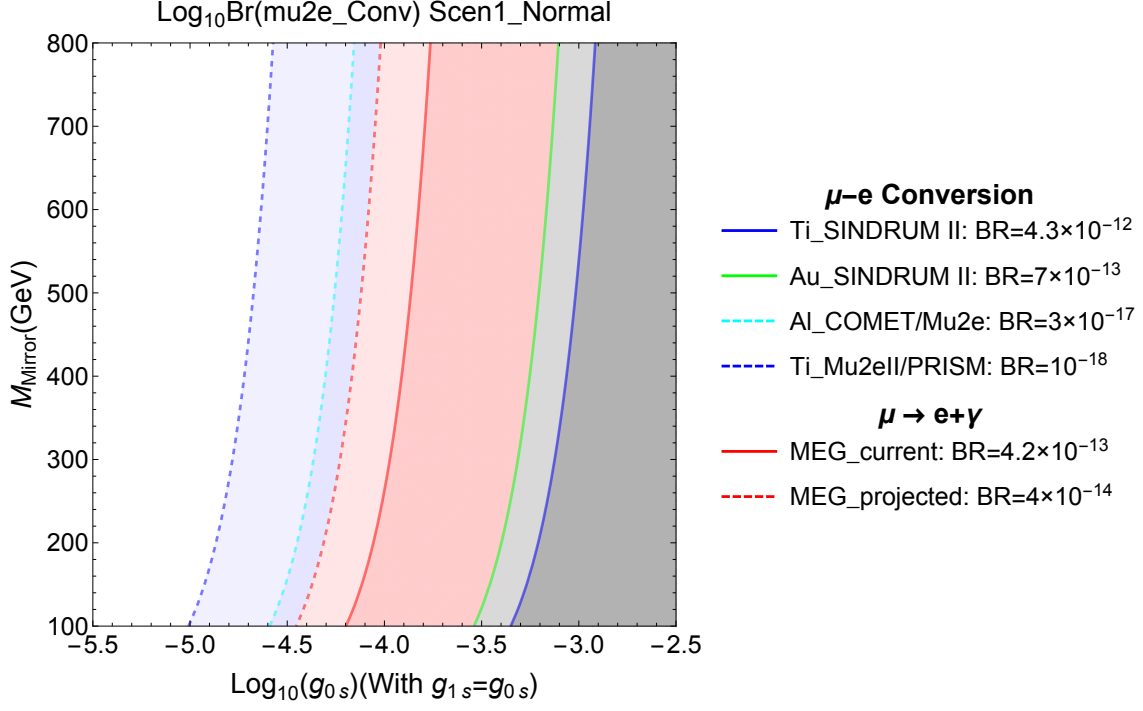


FIG. 4. Contour plots of $\text{Log}_{10} B(\mu - e \text{ conversion})$ on the $(g_{0S}, M_{\text{mirror}})$ plane for normal mass hierarchy in Scenarios 1 with $g_{0S} = g'_{0S} = g_{1S} = g'_{1S}$

- For the sensitivity of the two scenarios, we find that
 - Generally, Scenario 2 is less stringent constraint than Scenario 1.
 - In particular, when the A_4 singlet couplings are dominated, Scenario 2 is less stringent than Scenario 1 by at least two order of magnitude (10^{-3} vs. 10^{-1}), regarding the constraint on the couplings (as shown in Figs. 2 and 3). This is due to the fact that in Scenario 2, the three unknown unitary mixing matrices are now departure from U_{PMNS} which allows for larger effects since the amplitudes involve products of both the couplings and the elements of mixing matrices.

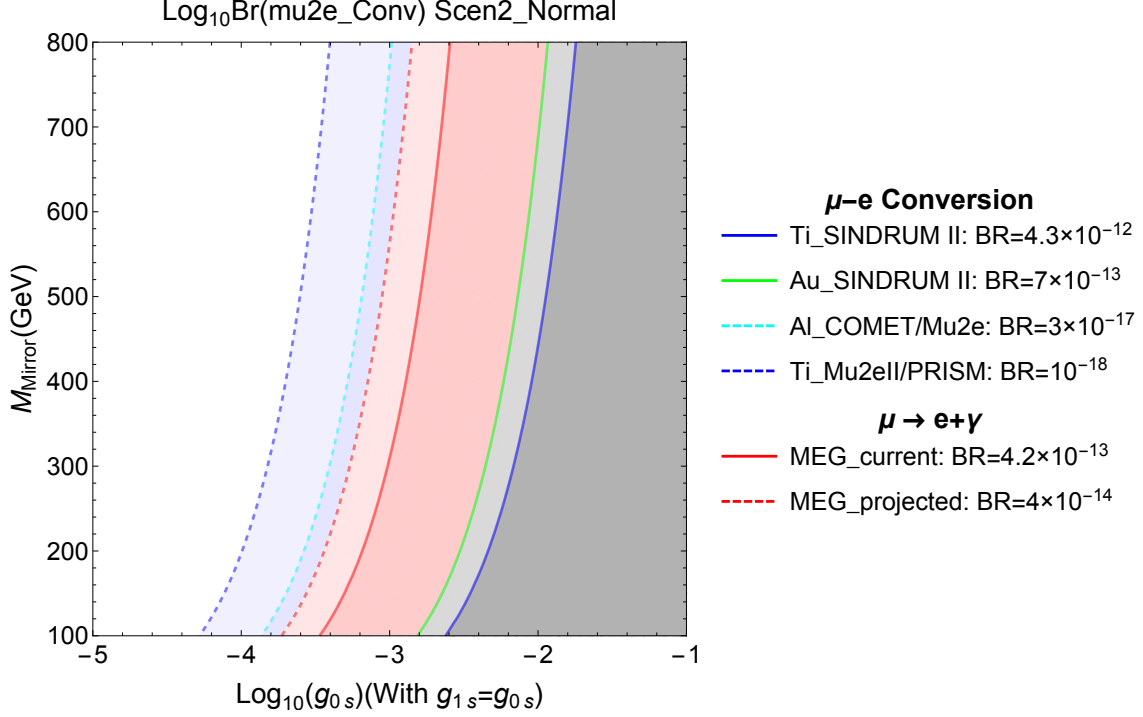


FIG. 5. Contour plots of $\text{Log}_{10} B(\mu - e \text{ conversion})$ on the $(g_{0S}, M_{\text{mirror}})$ plane for normal mass hierarchy in Scenarios 2 with $g_{0S} = g'_{0S} = g_{1S} = g'_{1S}$

- However, as one turns on the contribution from the A_4 triplet in Fig. (4) and Fig. (5), the discrepancy between two scenarios 1 and 2 shrink (10^{-2} vs. $10^{-3.2}$). It implies that Scenario 2 is more sensitive to the change in the structure of A_4 couplings.
- Finally, regarding the incorporation of the current limit on $B(\mu \rightarrow e\gamma)$ from MEG experiment and its projected sensitivity into the contour plots of $\log_{10} B(\mu - e \text{ conversion})$, one can obtain the following statements by looking at Figs. (2)-(5):
 - The plots illustrate nicely the close relation between the two CLFV pro-

cesses $\mu \rightarrow e\gamma$ and $\mu - e$ conversion in nuclei using the simple formula (45) we derived in Sec. III.

- In the same parameter space, $\mu \rightarrow e\gamma$ shows a tighter constraint than $\mu - e$ conversion by the fact that it excludes almost half of the searched region for the branching ratio of $\mu - e$ conversion. Therefore, our work helps narrow down future searches for $\mu - e$ conversion at Fermilab/Mu2e, J-PARC/COMET and PRISM.
- With the current upper bounds from various experiments, the radiative decay $\mu \rightarrow e\gamma$ is providing more stringent constraints on the couplings than the $\mu - e$ conversion (10^{-4} vs. 10^{-3} , about one order of magnitude better). However, for the future projected sensitivities at Mu2e and COMET, $\mu - e$ conversion is slightly more stringent, about half an order of magnitude stronger constraints on the couplings. For PRISM, it can be about an order of magnitude more stronger.

V. SUMMARY

Mirror fermion model with electroweak scale non-sterile right-handed neutrinos is an interesting extension of the SM. Aside from its aesthetically appealing to restoring parity symmetry at higher energy scale, it can have immediate impacts for experiments in both complementary frontiers of high energy and high intensity searching for new physics of lepton flavor violation.

In this study, we discussed $\mu - e$ conversion in nuclei and radiative decay $\mu \rightarrow e\gamma$ in an extended mirror fermion model with a A_4 horizontal symmetry in the lepton sector. Currently the most stringent constraint on the parameter space of the model is provided by the most recent limit on the radiative decay $\mu \rightarrow e\gamma$ from MEG. In

the future, Mu2e and COMET experiments can provide more stringent constraints on the model from $\mu - e$ conversion in aluminum. The sensitivity of the new Yukawa couplings can be probed is of order 10^{-5} , about one order of magnitude improvement compared with current status from MEG. Small Yukawa couplings such as 10^{-5} can give rise to distinct signatures in the search of mirror charged leptons and Majorana right-handed neutrinos at the LHC (or planned colliders) in the form of displaced decay vertices with decay lengths larger than 1 mm or so [28]. Although unrelated to the present analysis, a similar remark can be made for the search for mirror quarks [29].

It would be interesting to extend this study to the electric dipole moment of the electron and neutron, which requires the new Yukawa couplings to take on complex values instead of real ones as assumed in the present analysis. This work is in progress and will be presented elsewhere [37].

APPENDIX A - EFFECTIVE LAGRANGIAN FOR $\mu - e$ CONVERSION

Effective Lagrangian is a powerful technique to analyze low energy processes like $\mu \rightarrow e$ conversion in nuclei since the momentum transfer q^2 is typically of the order $\mathcal{O}(m_\mu^2) \ll m_N^2$ for nucleus N . The most general CLFV effective Lagrangian which contributes to the $\mu - e$ conversion in nuclei has been studied by various groups [21, 22, 38]. At the scale Λ where the heavy particles (including particles beyond the SM as well as the heavy top, bottom and charm quarks) being integrated out, the relevant terms for the model we are studying are

$$\begin{aligned} \mathcal{L}_{\text{eff}} = & -\frac{1}{\Lambda^2} \left[(C_{DR} m_\mu \bar{e} \sigma^{\alpha\beta} P_L \mu + C_{DL} m_\mu \bar{e} \sigma^{\alpha\beta} P_R \mu) F_{\alpha\beta} \right. \\ & \left. + \sum_{q=u,d,s} \left(C_{VR}^{(q)} \bar{e} \gamma^\alpha P_R \mu + C_{VL}^{(q)} \bar{e} \gamma^\alpha P_L \mu \right) \bar{q} \gamma_\alpha q + \text{H.c.} \right]. \end{aligned} \quad (48)$$

Here m_μ is the muon mass; $P_{L,R} = (1 \mp \gamma_5)/2$, $\sigma_{\mu\nu} = i[\gamma_\mu, \gamma_\nu]/2$; $F_{\alpha\beta}$ is the electromagnetic field strength; finally, $C_{D(L,R)}$ and $C_{V(L,R)}^{(q)}$ are dimensionless coupling constants depending on specific LFV model. In the specific mirror model calculation, we will be focusing on the photon and Z boson exchange diagrams which contribute only to the magnetic and electric dipole moment operators as well as the vector and axial vector lepton bilinears.

To determine the conversion rate, the above effective Lagrangian (48) is needed to scale down to the nuclear scale where the hadronic matrix elements $\langle N | \bar{q} \gamma_\mu q | N \rangle$, $\langle N | F^{\alpha\beta} F_{\alpha\beta} | N \rangle$ are evaluated. In addition, the muon and electron wave functions may be significantly deviated from plane wave due to distortion by the coulomb potential of the nuclei. For high Z nuclei, relativistic corrections to their wave functions are important as well. The formula for the conversion rate is given by [22, 38]

$$\Gamma_{\text{conv}} = \frac{m_\mu^5}{4\Lambda^4} \left(\left| C_{DR} D + 4\tilde{C}_{VR}^{(p)} V^{(p)} + 4\tilde{C}_{VR}^{(n)} V^{(n)} \right|^2 + \left| C_{DL} D + 4\tilde{C}_{VL}^{(p)} V^{(p)} + 4\tilde{C}_{VL}^{(n)} V^{(n)} \right|^2 \right). \quad (49)$$

TABLE III. Values of the dimensionless overlap integrals for aluminum, titanium and gold, evaluated under the assumption that the proton and neutron distributions within each nuclei are the same [22].

Nucleus	D	$V^{(p)}$	$V^{(n)}$
$^{27}_{13}\text{Al}$	0.0362	0.0161	0.0173
$^{48}_{22}\text{Ti}$	0.0864	0.0396	0.0468
$^{197}_{79}\text{Au}$	0.189	0.0974	0.146

In (49) the coupling constants $\tilde{C}_{V(R,L)}^{(p,n)}$ are defined as [38]

$$\tilde{C}_{VR}^{(p)} = \sum_{q=u,d,s} C_{VR}^{(q)} f_{Vp}^{(q)} , \quad (50)$$

$$\tilde{C}_{VR}^{(n)} = \sum_{q=u,d,s} C_{VR}^{(q)} f_{Vn}^{(q)} , \quad (51)$$

$$\tilde{C}_{VL}^{(p)} = \sum_{q=u,d,s} C_{VL}^{(q)} f_{Vp}^{(q)} , \quad (52)$$

$$\tilde{C}_{VL}^{(n)} = \sum_{q=u,d,s} C_{VL}^{(q)} f_{Vn}^{(q)} , \quad (53)$$

where $f_{Vp}^{(q)}$ and $f_{Vn}^{(q)}$ are the known nucleon vector form factors

$$\begin{aligned} f_{Vp}^{(u)} &= 2, \quad f_{Vp}^{(d)} = 1, \quad f_{Vp}^{(s)} = 0 , \\ f_{Vn}^{(u)} &= 1, \quad f_{Vn}^{(d)} = 2, \quad f_{Vn}^{(s)} = 0 . \end{aligned} \quad (54)$$

The dimensionless quantities D and $V^{(p,n)}$ in (49) are the overlap integrals of the relativistic wave functions of muon and electron in the electric field of the nucleus weighted by appropriate combinations of proton and neutron densities [22]. Their values for the four nuclei aluminum, titanium, gold and lead are listed in Table III for reference.

TABLE IV. Standard model values of the capture rates for aluminum, titanium and gold in unit of 10^6 s^{-1} taken from Ref. [39].

Nucleus $\Gamma_{\text{capt}} (10^6 \text{ s}^{-1})$	
$^{27}_{13}\text{Al}$	0.7054
$^{48}_{22}\text{Ti}$	2.59
$^{197}_{79}\text{Au}$	13.07

The $\mu - e$ conversion branching ratio is defined as

$$B_{\mu N \rightarrow e N}(Z, A) \equiv \frac{\Gamma_{\text{conv}}}{\Gamma_{\text{capt}}} , \quad (55)$$

where Γ_{conv} is given by (49) and Γ_{capt} is the standard model muon capture rate. The SM capture rates for aluminum, titanium and gold have been determined experimentally [39] and they are listed in Table IV for convenience.

APPENDIX B - FORMULAS FOR $\mathcal{I}, \mathcal{J}, \mathcal{I}_{i0} (i = 1, \dots, 5)$

In the limit of zero momentum transfer, the Feynman parameterization integrals in the various form factors can be carried out analytically. We collect their results here.

$$\mathcal{I}(r) = \frac{1}{12(1-r)^4} [-6r^2 \log r + r(2r^2 + 3r - 6) + 1] , \quad (56)$$

$$\mathcal{J}(r) = \frac{1}{2(1-r)^3} [-2r^2 \log r + r(3r - 4) + 1] , \quad (57)$$

$$\mathcal{I}_{10}(r) = \frac{1}{72(1-r)^6} [-12r^2(3+2r) \log r + (r-1)(3r^3 + 47r^2 + 11r - 1)] , \quad (58)$$

$$\mathcal{I}_{20}(r) = \frac{1}{36(1-r)^5} [-6r^2(3+r) \log r + (r-1)(17r^2 + 8r - 1)] , \quad (59)$$

$$\mathcal{I}_{30}(r) = \frac{1}{36(1-r)^4} [6r^3 \log r + (-11r^2 + 18r - 9)r + 2] , \quad (60)$$

$$\mathcal{I}_{40}(r) = \frac{1}{144(1-r)^6} [12r^3(r+4) \log r - (r^2 - 1)(37r^2 - 8r + 1)] , \quad (61)$$

$$\mathcal{I}_{50}(r) = \frac{1}{18(1-r)^5} [12r^3 \log r - (3r^4 + 10r^3 - 18r^2 + 6r) + 1] . \quad (62)$$

Here r denotes the mass ratio m^2/M^2 , where m and M are the masses of the scalar singlet and mirror lepton respectively.

ACKNOWLEDGMENTS

TCY would like to thank T. N. Pham for useful discussions and the hospitality he received at Centre de Physique Théorique de l'Ecole Polytechnique where progress of this project was made. We would also like to thank Craig Group for useful comments on the manuscript. This work was supported in part by the Ministry of Science and Technology (MoST) of Taiwan under grant number 104-2112-M-001-001-MY3.

-
- [1] S. T. Petcov, “The Processes $\mu \rightarrow e \gamma$, $\mu \rightarrow e e \text{ anti-}e$, Neutrino’ \rightarrow Neutrino γ in the Weinberg-Salam Model with Neutrino Mixing,” *Sov. J. Nucl. Phys.* **25**, 340 (1977) [*Yad. Fiz.* **25**, 641 (1977)] Erratum: [*Sov. J. Nucl. Phys.* **25**, 698 (1977)] Erratum: [*Yad. Fiz.* **25**, 1336 (1977)].
 - [2] E. Ma and A. Pramudita, “Exact Formula for $(\mu \rightarrow e \gamma)$ Type Processes in the Standard Model,” *Phys. Rev. D* **24**, 1410 (1981).
 - [3] A. M. Baldini *et al.* [MEG Collaboration], “Search for the Lepton Flavour Violating Decay $\mu^+ \rightarrow e^+ \gamma$ with the Full Dataset of the MEG Experiment,” *Eur. Phys. J. C* **76**, no. 8, 434 (2016) [arXiv:1605.05081 [hep-ex]].
 - [4] F. Renga [MEG Collaboration], “Latest results of MEG and status of MEG-II,” arXiv:1410.4705 [hep-ex].
 - [5] See the talk presented by K. Iwamoto (T2K Collaboration) at the ICHEP 2016, Chicago, August 2016.
 - [6] M. C. Gonzalez-Garcia, M. Maltoni and T. Schwetz, “Global Analyses of Neutrino Oscillation Experiments,” *Nucl. Phys. B* **908**, 199 (2016) [arXiv:1512.06856 [hep-ph]].
 - [7] P. Adamson *et al.* [NOvA Collaboration], “First measurement of electron neutrino appearance in NOvA,” *Phys. Rev. Lett.* **116**, no. 15, 151806 (2016) [arXiv:1601.05022]

- [hep-ex]].
- [8] P. Adamson *et al.* [NOvA Collaboration], “First measurement of muon-neutrino disappearance in NOvA,” *Phys. Rev. D* **93**, no. 5, 051104 (2016) [arXiv:1601.05037 [hep-ex]].
 - [9] C. Dohmen *et al.* [SINDRUM II Collaboration], “Test of lepton-flavour conservation in $\mu - e$ conversion on titanium,” *Phys. Lett. B* **317** (1993) 631.
 - [10] W. H. Bertl *et al.* [SINDRUM II Collaboration], “A Search for muon to electron conversion in muonic gold,” *Eur. Phys. J. C* **47**, 337 (2006).
 - [11] L. Bartoszek *et al.* [Mu2e Collaboration], “Mu2e Technical Design Report,” arXiv:1501.05241 [physics.ins-det].
 - [12] Y. Kuno [COMET Collaboration], “A search for muon-to-electron conversion at J-PARC: The COMET experiment,” *PTEP* **2013**, 022C01 (2013).
 - [13] COMET Collaboration, Technical Design Report (2016).
 - [14] K. Knoepfel *et al.* [Mu2e Collaboration], “Feasibility Study for a Next-Generation Mu2e Experiment,” arXiv:1307.1168 [physics.ins-det].
 - [15] R. J. Barlow, “The PRISM/PRIME project,” *Nucl. Phys. Proc. Suppl.* **218**, 44 (2011).
 - [16] M. Lindner, M. Platscher and F. S. Queiroz, “A Call for New Physics : The Muon Anomalous Magnetic Moment and Lepton Flavor Violation,” arXiv:1610.06587 [hep-ph].
 - [17] P. Q. Hung, T. Le, V. Q. Tran and T. C. Yuan, “Lepton Flavor Violating Radiative Decays in EW-Scale ν_R Model: An Update,” *JHEP* **1512**, 169 (2015) [arXiv:1508.07016 [hep-ph]].
 - [18] P. Q. Hung, “Electroweak-scale mirror fermions, $\mu \rightarrow e\gamma$ and $\tau \rightarrow \mu\gamma$,” *Phys. Lett. B* **659**, 585 (2008) [arXiv:0711.0733 [hep-ph]].
 - [19] P. Q. Hung, “A Model of electroweak-scale right-handed neutrino mass,” *Phys. Lett. B* **649**, 275 (2007) [hep-ph/0612004].

- [20] P. Q. Hung and T. Le, “On neutrino and charged lepton masses and mixings: A view from the electroweak-scale right-handed neutrino model,” *JHEP* **1509**, 001 (2015) [arXiv:1501.02538 [hep-ph]].
- [21] Y. Kuno and Y. Okada, “Muon decay and physics beyond the standard model,” *Rev. Mod. Phys.* **73**, 151 (2001) [hep-ph/9909265].
- [22] R. Kitano, M. Koike and Y. Okada, “Detailed calculation of lepton flavor violating muon electron conversion rate for various nuclei,” *Phys. Rev. D* **66**, 096002 (2002) Erratum: [*Phys. Rev. D* **76**, 059902 (2007)] [hep-ph/0203110].
- [23] J. C. Pati and A. Salam, “Lepton Number as the Fourth Color,” *Phys. Rev. D* **10**, 275 (1974) [*Phys. Rev. D* **11**, 703 (1975)].
- [24] R. N. Mohapatra and J. C. Pati, “A Natural Left-Right Symmetry,” *Phys. Rev. D* **11**, 2558 (1975).
- [25] G. Senjanovic and R. N. Mohapatra, “Exact Left-Right Symmetry and Spontaneous Violation of Parity,” *Phys. Rev. D* **12**, 1502 (1975).
- [26] G. Senjanovic, “Spontaneous Breakdown of Parity in a Class of Gauge Theories,” *Nucl. Phys. B* **153**, 334 (1979).
- [27] H. B. Nielsen and M. Ninomiya, “No Go Theorem for Regularizing Chiral Fermions,” *Phys. Lett.* **105B**, 219 (1981).
- [28] S. Chakdar, K. Ghosh, V. Hoang, P. Q. Hung and S. Nandi, “The search for electroweak-scale right-handed neutrinos and mirror charged leptons through like-sign dilepton signals,” to appear in *Phys. Rev. D* (2017) [arXiv:1606.08502 [hep-ph]].
- [29] S. Chakdar, K. Ghosh, V. Hoang, P. Q. Hung and S. Nandi, “Search for mirror quarks at the LHC,” *Phys. Rev. D* **93**, no. 3, 035007 (2016) [arXiv:1508.07318 [hep-ph]].
- [30] V. Hoang, P. Q. Hung and A. S. Kamat, “Electroweak precision constraints on the electroweak-scale right-handed neutrino model,” *Nucl. Phys. B* **877**, 190 (2013) [arXiv:1303.0428 [hep-ph]].

- [31] V. Hoang, P. Q. Hung and A. S. Kamat, “Non-sterile electroweak-scale right-handed neutrinos and the dual nature of the 125-GeV scalar,” Nucl. Phys. B **896**, 611 (2015) [arXiv:1412.0343 [hep-ph]].
- [32] H. Georgi and M. Machacek, “Doubly Charged Higgs Bosons,” Nucl. Phys. B **262**, 463 (1985).
- [33] M. S. Chanowitz and M. Golden, “Higgs Boson Triplets With $M(W) = M(Z) \cos \theta_W$,” Phys. Lett. B **165**, 105 (1985).
- [34] N. Cabibbo, “Time Reversal Violation in Neutrino Oscillation,” Phys. Lett. B **72**, 333 (1978).
- [35] L. Wolfenstein, “Oscillations Among Three Neutrino Types and CP Violation,” Phys. Rev. D **18**, 958 (1978).
- [36] E. Ma, “A(4) Symmetry and Neutrinos,” Int. J. Mod. Phys. A **23**, 3366 (2008) [arXiv:0710.3851 [hep-ph]]; E. Ma and G. Rajasekaran, “Softly broken A(4) symmetry for nearly degenerate neutrino masses,” Phys. Rev. D **64**, 113012 (2001) [hep-ph/0106291]. See also S. F. King and C. Luhn, “Neutrino Mass and Mixing with Discrete Symmetry,” Rept. Prog. Phys. **76**, 056201 (2013) [arXiv:1301.1340 [hep-ph]] for a review and references therein.
- [37] C. F. Chang, P. Q. Hung, C. S. Nugroho, V. Q. Tran, and T. C. Yuan, in preparation.
- [38] V. Cirigliano, R. Kitano, Y. Okada and P. Tuzon, “On the model discriminating power of $\mu - e$ conversion in nuclei,” Phys. Rev. D **80**, 013002 (2009) [arXiv:0904.0957 [hep-ph]].
- [39] T. Suzuki, D. F. Measday and J. P. Roalsvig, Phys. Rev. C **35**, 2212 (1987).